PAPER K

ACOUSTIC WAVE EQUATION TOMOGRAPHY USING A NEW MOMENT METHOD

Feng Yin and Jerry M. Harris

ABSTRACT

We review a new moment method of solving the acoustical scattering equation, and then apply this method to non-linear wave equation tomography. We describe the formulation, the implementaion, and numerical testing of the method. The main characteristic of this method is that a bilinear basis function is used instead of a pulse basis function to evaluate the Green function, total field, and scattering potential at any arbitray point of the image region. In this way, the integral equation may be discretized to arbitrary fineness in order to increase the accuracy of the computations. From simulation tests, we find that this method is accurate and the number of inversion unknowns can be greatly reduced. We utilize this method in solving a non-linear wave equation inverse problem.

INTRODUCTION

In recent years, some researchers made effort to apply the wave equation tomography to real data with mixed results. Some used the time-domain waveform data to invert for velocity; others used the frequency domain wave field. In frequency domain methods, the wave field in the inhomogenous media is required. There are two types of the methods useful for obtaining this wave field. One is to solve the wave equation in its derivative form, e.g., finite differences (Pratt, 1988), or boundary element methods (Barhe, 1982). Another is to solve the scattering integral equation, e.g., moment method using pulse basis function (Richmond, 1965). The moment method is especially useful for modeling the wave field in a local region of interest rather than a larger area as in finite difference methods. And with the moment method, the Frechet derivative for inversion is easy to derive.

However, it is known that pulse basis functions do not produce accurate representation with the method of moments for pixel sizes larger than about 0.1 wavelength. Therefore, for large scale imaging problems, we must invert a huge matrix in order to find the wave field in the inhomogenous media. This is the main problem of the moment method. Therefore, up to now, there are many authors who are attempting to improve this method (Johnson, 1983, Steinberg, 1993, Zhuck, 1994). To develop a more efficient numerical solution for the 2-D wave propagation in the inhomogeneous media, we develop a new variations on the moment method. In our method, we discretize the integral equation using bilinear basis functions instead of pulse basis functions.. In this way, we can not only increase the accuracy of the calculation of wave field, but also reduce the number of pixels representing the field. And from this method, the Frechet

derivative for non-linear wave equation inversion is easy to derive. Then we apply this method to non-linear wave equation inversion and test the validity of the method.

A NEW MOMENT METHOD FOR SOLVING SCATTERING EQUATION

In this paper, we restrict ourselves to the acoustic wave propagation in 2-D inhomogeneous media..In the frequency domain, we have:

$$(\nabla^2 + \frac{\omega^2}{c^2(\boldsymbol{r})})u(\boldsymbol{r},\omega) = -\delta(\boldsymbol{r}-\boldsymbol{r}_s) \tag{1}$$

where, $c(\boldsymbol{r})$ is the velocity of the compressional wave, $\mathbf{r}$ is the position vector, $u(\boldsymbol{r},\omega)$ is the pressure, and ω is the angle frequency. Let us define

$$M(\boldsymbol{r}) = 1 - \frac{c_0^2}{c^2(\boldsymbol{r})} \tag{2}$$

and let

$$u(\boldsymbol{r}) = u^i(\boldsymbol{r}) + u^s(\boldsymbol{r}), \tag{3}$$

then the integral equation corresponding to Eqn. (1) can be written

$$u(\boldsymbol{r}) = u^i(\boldsymbol{r}) - k^2 \int_{\Omega} M(\boldsymbol{r}')u(\boldsymbol{r}',\omega)G(k|\boldsymbol{r}-\boldsymbol{r}'|)d\boldsymbol{r}' \tag{4}$$

where $k = \omega/c_0$, Ω is the object region. As shown in Figure 1, the object region is divided into L_a pixels with N nodes, that is, $\Omega = \Omega_1 \cup \Omega_2 \cdots \cup \Omega_{L_a}, \Omega_i \cup \Omega_j (i \neq j)$.

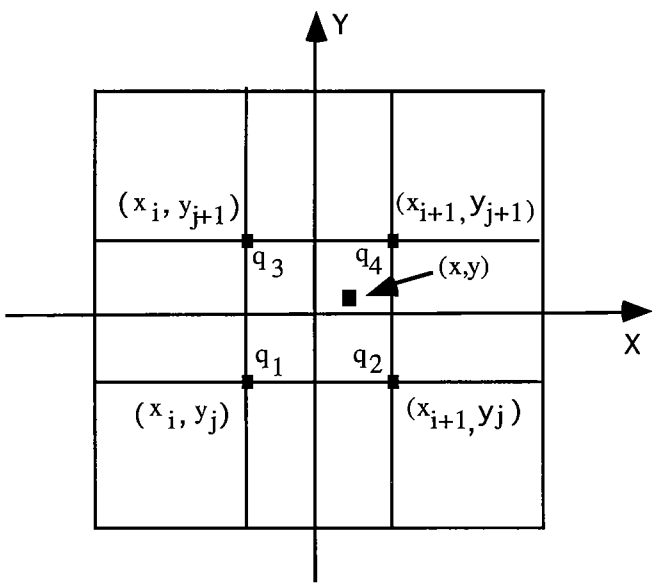

Figure 1: The discretized form of the object region. q1,q2.q3 and q4 denote the nodes (x_i,y_j), (x_{i+1},y_j), (x_i,y_{j+1}) and (x_{i+1},y_{j+1})

We then have

$$u(\boldsymbol{r}) = u^{i}(\boldsymbol{r}) - k^{2} \sum_{i=1}^{L_a} \int_{\Omega_i} M(\boldsymbol{r}')u(\boldsymbol{r}', \omega)G(k|\boldsymbol{r} - \boldsymbol{r}'|)d\boldsymbol{r}'. \tag{5}$$

When $\boldsymbol{r}'$ is located in Ω_i, $(x_i,y_j),(x_{i+1},y_j),(x_i,y_{j+1}),(x_{i+1},y_{j+1})$ are used to denote the four nodes of the cell Ω_i as shown in Figure 1. We use (x,y) to denote a point within the cell; Δx and Δy are the intervals of x and y directions, respectively. When $x_i \le x \le x_{i+1}$, $y_i \le y \le y_{i+1}$, define

$$\rho_{ip} = \begin{cases} f_1 & ip = (j-1) \times mx + i \\ f_2 & ip = (j-1) \times mx + i + 1 \\ f_3 & \text{when} \quad ip = (j-1) \times mx + i + mx \\ f_4 & ip = (j-1) \times mx + i + mx + 1 \\ 0 & ip = others \end{cases} \tag{6}$$

where mx is the total numbers of the nodes in the x direction.

$$f_1 = 1 - \frac{(x - x_i)}{\Delta x} - \frac{(y - y_i)}{\Delta y} - \frac{(x - x_i)(y - y_j)}{\Delta x \Delta y} \tag{7}$$

$$f_2 = \frac{(x - x_i)}{\Delta x} - \frac{(x - x_i)(y - y_j)}{\Delta x \Delta y} \tag{8}$$

$$f_3 = \frac{(y - y_i)}{\Delta y} - \frac{(x - x_i)(y - y_j)}{\Delta x \Delta y} \tag{9}$$

$$f_4 = \frac{(x - x_i)(y - y_j)}{\Delta x \Delta y} \tag{10}$$

$M(\boldsymbol{r})$, $u(\boldsymbol{r})$ and $G(\boldsymbol{r};\boldsymbol{r}',k)$ are expanded using the basis function $\{\rho_{ip}(x,y)\}$. We have

$$M(\boldsymbol{r}) = \sum_{l=1}^{N} \rho_l \cdot M_l \tag{11}$$

$$u(\boldsymbol{r},k) = \sum_{n=1}^{N} \rho_n u_n \tag{12}$$

$$G(\boldsymbol{r};\boldsymbol{r}',k) = \sum_{m=1}^{N} \rho_m \cdot G_m \tag{13}$$

where N is the total number of the nodes in the object area; O_l,, u_n, and G_m represent the value of $M(\boldsymbol{r})$ at the lth node, $u(\boldsymbol{r},k)$ at nth node, and $G(\boldsymbol{r};\boldsymbol{r}')$ at mth node in row order, respectively.

For the sake of simplicity, q1, q2, q3 and q4 are used to represent the nodes $(x_i, y_j), (x_{i+1}, y_j), (x_i, y_{j+1})$ and (x_{i+1}, y_{j+1}), respectively. Integrating Eqns (11)-(13) into equation (4), we obtain

$$\sum_{l=1}^{N} A_{jl} u_l = u_l^i \tag{14}$$

where N is total number of the nodes, and when $l \neq j, l \neq j-1, l \neq j-mx-1$, $l \neq j-mx-2$, and

$$A_{jl} = -k^2 (B_l H^{(1)}_{l,La+1} + C_l H^{(2)}_{l,2} H^{(1)}_{l,La-2} + D_l H^{(2)}_{l,mx-1} H^{(1)}_{l,L_a-mx-1} + E_l H^{(2)}_{l,mx-2}) \tag{15}$$

In above equation

$$H^{(1)}_{l,l'} = \begin{cases} 1 & l < l' \\ 0 & l \geq l' \end{cases} \tag{16}$$

$$H^{(2)}_{l,l'} = \begin{cases} 0 & l < l' \\ 1 & l \geq l' \end{cases} \tag{17}$$

$$\begin{aligned} B_l = \{&\tfrac{1}{16} Q_1(q_1) Q_2(q_1) + \tfrac{1}{48} [Q_1(q_2) Q_2(q_2) + Q_1(q_3) Q_2(q_3) + Q_1(q_2) Q_2(q_1) + \\ &Q_1(q_1) Q_2(q_2) + Q_1(q_3) Q_2(q_1) + Q_1(q_1) Q_2(q_3)] + \tfrac{1}{144} [Q_1(q_4) Q_2(q_4) + \\ &Q_1(q_4) Q_2(q_1) + Q_1(q_4) Q_2(q_3) + Q_1(q_1) Q_2(q_4) + Q_1(q_2) Q_2(q_3) + \\ &Q_1(q_2) Q_2(q_4) + Q_1(q_3) Q_2(q_2) + Q_1(q_3) Q_2(q_4) + Q_1(q_4) Q_2(q_2)]\} \Delta x \Delta y \end{aligned} \tag{18}$$

$$\begin{aligned} C_l = \{&\tfrac{1}{16} Q_1(q_2) Q_2(q_2) + \tfrac{1}{48} [Q_1(q_1) Q_2(q_1) + Q_1(q_4) Q_2(q_4) + Q_1(q_2) Q_2(q_1) + \\ &Q_1(q_1) Q_2(q_2) + Q_1(q_4) Q_2(q_2) + Q_1(q_2) Q_2(q_4)] + \tfrac{1}{144} [Q_1(q_3) Q_2(q_3) + \\ &Q_1(q_3) Q_2(q_1) + Q_1(q_1) Q_2(q_3) + Q_1(q_4) Q_2(q_1) + Q_1(q_1) Q_2(q_4) + \\ &Q_1(q_2) Q_2(q_3) + Q_1(q_3) Q_2(q_2) + Q_1(q_4) Q_2(q_3) + Q_1(q_3) Q_2(q_4)]\} \Delta x \Delta y \end{aligned} \tag{19}$$

$$\begin{aligned} D_l = \{&\tfrac{1}{16} Q_1(q_3) Q_2(q_3) + \tfrac{1}{48} [Q_1(q_1) Q_2(q_1) + Q_1(q_4) Q_2(q_4) + Q_1(q_4) Q_2(q_3) + \\ &Q_1(q_3) Q_2(q_4) + Q_1(q_3) Q_2(q_1) + Q_1(q_1) Q_2(q_3)] + \tfrac{1}{144} [Q_1(q_2) Q_2(q_2) + \\ &Q_1(q_2) Q_2(q_1) + Q_1(q_1) Q_2(q_4) + Q_1(q_2) Q_2(q_3) + Q_1(q_1) Q_2(q_2) + \\ &Q_1(q_4) Q_2(q_1) + Q_1(q_3) Q_2(q_2) + Q_1(q_4) Q_2(q_2) + Q_1(q_2) Q_2(q_4)]\} \Delta x \Delta y \end{aligned} \tag{20}$$

and

$$\begin{aligned} E_l = \{&\tfrac{1}{16}Q_1(q_4)Q_2(q_4)+\tfrac{1}{48}[Q_1(q_2)Q_2(q_2)+Q_1(q_3)Q_2(q_3)+Q_1(q_2)Q_2(q_4)+\\ &Q_1(q_4)Q_2(q_3)+Q_1(q_4)Q_2(q_2)+Q_1(q_3)Q_2(q_4)]+\tfrac{1}{144}[Q_1(q_2)Q_2(q_1)+\\ &Q_1(q_1)Q_2(q_4)+Q_1(q_1)Q_2(q_2)+Q_1(q_1)Q_2(q_3)+Q_1(q_4)Q_2(q_1)+\\ &Q_1(q_3)Q_2(q_1)+Q_1(q_3)Q_2(q_2)+Q_1(q_1)Q_2(q_1)+Q_1(q_2)Q_2(q_3)]\}\Delta x\Delta y \end{aligned} \tag{21}$$

where $Q_1(q_i)=G_{q_i}$ and $Q_2(q_i)=M_{q_i}$.when $(l=j, l=j-1, l=j-mx-1, l=j-mx-2)$

$$A_{jl}=\frac{i}{2}[\pi kaH_0^{(1)}(ka)+2i]*M_l \tag{22}$$

where a=$\sqrt{\Delta x\cdot\Delta y/\pi}$. Thus, equation (14) can be written as

$$\boldsymbol{AU}=\boldsymbol{U}^i \tag{23}$$

where $\boldsymbol{U}=(u_1,u_2,\cdots,u_N)^t, \boldsymbol{U}^i=(u_1^i,u_2^i,\cdots,u_N^i)^t$, Therefore, the total field can be obtained by solving equation (23), we have

$$\boldsymbol{U}=\boldsymbol{A}^{-1}\boldsymbol{U}^i \tag{24}$$

After the total field is solved, the scattering field at r_m outside the object region can be expressed as

$$u_m^s=\sum_{l=1}^{N}A_{ml}M_l \tag{25}$$

where A_{ml} equals to equation (14), and $Q_1(q_i)=G(q_i), Q_2(q_i)=u(q_i)$. Therefore, the scattering field in frequency domain can be derived by equation (24) and the waveform of the scattering can be derived by applying inverse Fourier transform to the wave field in the fequency domain.

APPLICATION TO NON-LINEAR WAVE EQUATION INVERSION

Suppose now that the observed wave field is $U^0(\mathbf{r}_s,\mathbf{r}_s,\omega)$ $(1\le s\le S, 1\le g\le G)$. We wish to use these observed data to determine a model M=$(m_1,m_2,\cdots,m_N)$ from which the corresponding calculated wave field matches the observed wave field. Therefore, we should have a measure of fit, that is, we should establish a measure for assessing the degree of mismatch between the observed data and the synthetic data. We choose the squared L2 norm of the observed and calculated data. That is, our goal is to minimize the function

$$J(M)=\tfrac{1}{2}\sum_{s}^{S}\sum_{g}^{G}\|U^O(r_S,r_g,\omega)-U^C(r_S,r_g,\omega)\|^2=\text{minimum} \tag{26}$$

where U^o and U^c are measured field data and calculated field data, respectively. The wave equation inverse problem in crosswell geometry is not only nonlinear, but extremely non unique, that is, ill-posed. In order to derive a stable solution of the inverse problem and prevent unrealistic behavior of the model parameters, we impose a form of regularization on Eqn. (26) as follows:

$$Q(\mathbf{M}) = \frac{1}{2}\sum_{s}^{S}\sum_{g}^{G}\|U^o(r_s,r_g,\omega) - U^c(r_s,r_g,\omega)\|^2 + \lambda H(\mathbf{M}) = \text{minimum} \quad (27)$$

where H(M) is the regularization term, e.g., a smoothing operator. Then, we use a steepest gradient method, conjugate gradients to solve (27). Eqn. (27) is quadratic, therefore, not only the first derivative, but also the second derivative is required. A subspace method (Kennet, etc., 1987, Skilling, et al, 1987) in which the Hessian matrix is used will be utilized to solve Eqn. (27).

In the subspace method, the current model is updated by a small model perturbation which is determined in a small subspace, that is

$$\mathbf{M}^{(q+1)} = \mathbf{M}^{(q)} + \Delta\mathbf{M}^{(q)} \quad (28)$$

$$\Delta\mathbf{M}^{(q)} = x_1\mathbf{e}_1 + x_2\mathbf{e}_2 + x_3\mathbf{e}_3 \quad (29)$$

where $\mathbf{e}_1, \mathbf{e}_2$ and $\mathbf{e}_3$ are the basis of the subspace, and they are

$$(\mathbf{e}_1)_i = \frac{\partial J}{\partial m_i},\ (\mathbf{e}_2)_i = \frac{\partial H}{\partial m_i},\ (\mathbf{e}_3)_i = \sum_k \frac{\partial^2 J}{\partial m_i \partial m_k}\frac{\partial Q}{\partial m_k} \quad (30)$$

and x_1, x_2 and x_3 can be determined by the subspace method (Skilling,1984, Kennet, et al, 1987).

We can see that one of main points of the inversion step is the calculation of the Frechét derivative and the second derivative of the quadratic function. After the wave fields are calculated in the current background media, the total wave field at receiver array can be derived by equation (25):

$$U\ (\mathbf{r}_s,\mathbf{r}_g,\omega) = U^i(\mathbf{r}_s,\mathbf{r}_g,\omega) + \sum_j A_{ji}m_i\ \ (j = 1,\cdots,G\cdot S) \quad (31)$$

The Frechét derivative for inversion and the second derivative of the objective function can be easily expressed as

$$\frac{\partial J}{\partial m_i} = \sum_{l}^{SGL} R(A_{li})\cdot\left[R(U_l^c) - R(U_l^o)\right] + I(A_{li})\cdot\left[I(U_l^c) - I(U_l^o)\right] \quad (32)$$

$$\frac{\partial^2 J}{\partial m_i \partial m_k} = \sum_{l}^{SGL}[R(A_{li})\cdot R(A_{lk}) + I(A_{li})\cdot R(A_{lk})] \quad (33)$$

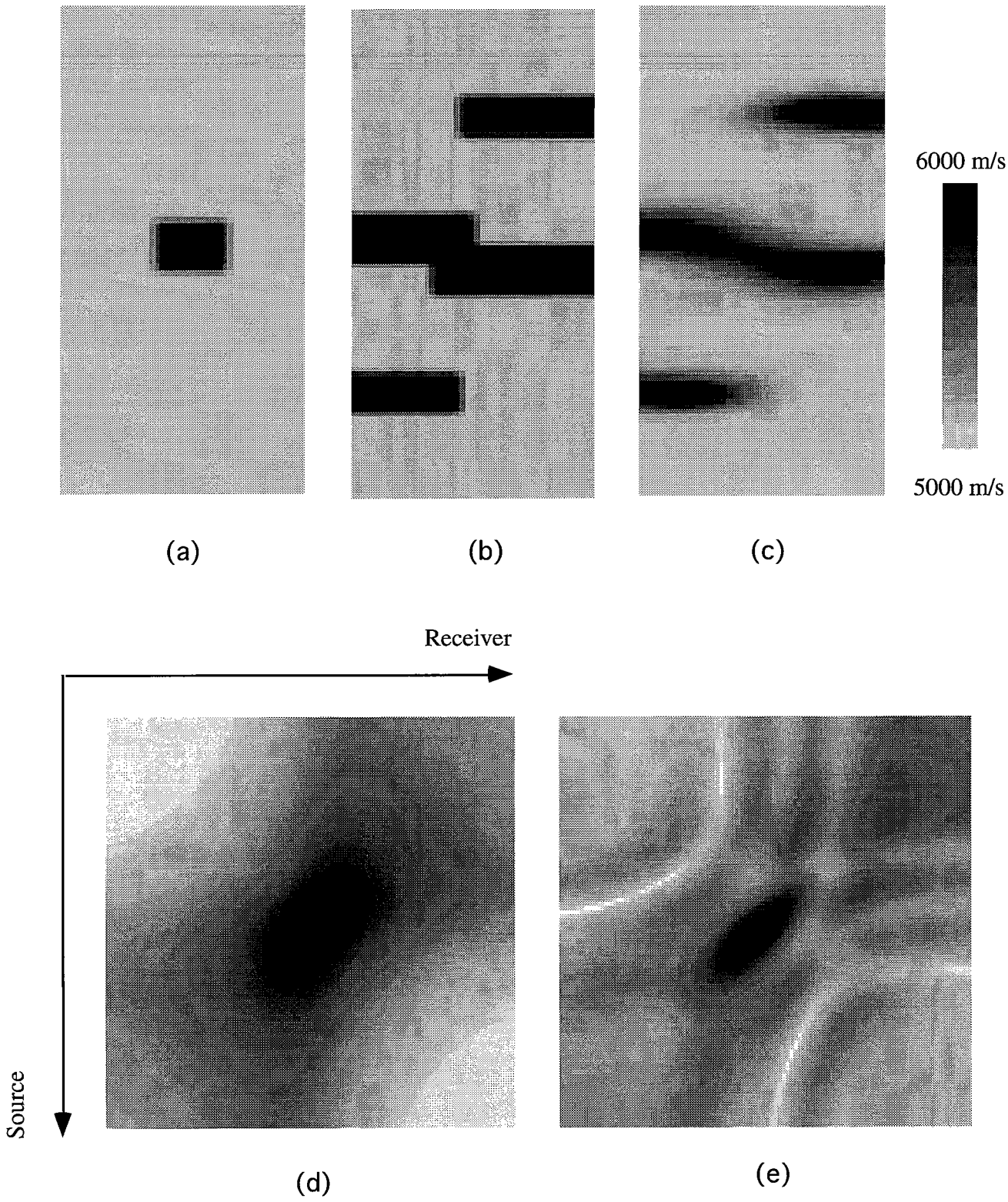

Figure 2. (a) Synthetic model I. (b) Synthetic model II. (c) Reconstructed result of model II. (d) Amplitude of scattered field of model I. (e) Amplitude of scattered field of model II

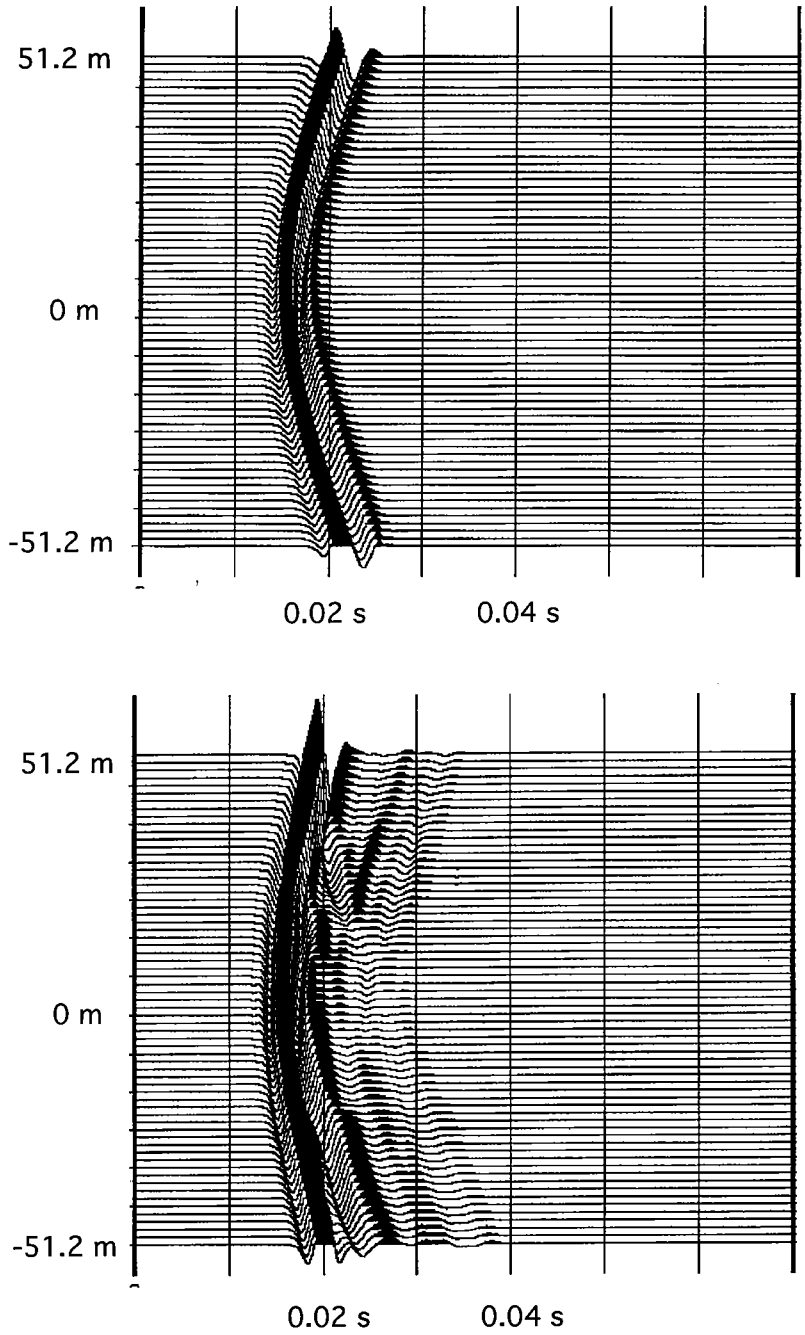

Figure 3: (a) The waveform of the scattered field by model I. (b) The waveform of the scattered field by model II

where R and I means taking real part and imaginary part. S, G, and L are the total number of the discrete sources, receivers, and frequencies, and up-script c and o mean the calculated and measured value.

Because analytical formulas for the Frechét derivative can be obtained for our numerical method, we use them to invert the model by non-linear iterative methods of

Eqns. (29). This is one of the advantages of using the integral equation over the differential equation.

NUMERICAL SIMULATIONS

Figures 2 (a) and (b) are two models for forward calculation. The velocities are denoted in the pictures. We locate 100 sources at x=-30 m in equal depth Δs=1.6 m, and put 100 receivers at x=+30 m in equal depth Δr=1.6 m. Figures 2 (c) and (d) are the amplitudes of the scattering wave field corresponding to the models using out moment method. In order to test our method effectively, we also applied this forward method to the nonlinear wave equation inversion, figure 2 (e) is the reconstructed result by our moment inversion method. Finally, we applied inverse Fourire transform to the scattering field in frequency domain to obtain the waveform of the scattering field. Figures 3 (a) and (b) are the scattering waveforms of one common shot gather where a ricker wavelet of 300 Hz center frequency is used and the $\Delta x = \Delta y = 1/6$ $\Delta x = \Delta y = 1/6 \times \lambda_{\min}$.

CONCLUSIONS

We reviewed a new moment method for evaluating the wave field in the inhomogeneous media in this paper. With this method, the wave field not only can be calculated accurately when there are 6 nodes per wavelength instead of 10 pixels per wavelength with the pulse basis function. Also, the Frechet derivative is easy to derive for non-linear wave equation inversion. Computer simulations show our method is effective and very useful in solving both forward and inverse problems.

ACKNOWLEDGMENTS

This work is supported by the Seismic Tomography Project of Stanford University, a research consortium sponsored by companies of the oil and gas industry.

REFERENCES

Bathe, K.J., Finite Element Procedures in Engineering Analysis, Englewood Cliffs, NJ: Prentice Hall, Inc., 1982

Ben Zion and Yehuda Leviatan, On the use of Wavelet Expansions in the method of moments, IEEE Transaction on antennas and propagation, vol. 41, no.5, 1993

Nickolay P. Zhuck and Alexander G. Yarovoy, Two-dimensional scattering from an inhomogeneous dielectric cylinder embedded in a stratified medium: Case of TM polarization, IEEE Transaction on antennas and propagation, vol. 42, no.1, 1994.

Pratt, R.G., Frequency-domain elastic wave modeling by finite differences: A tool for crosshole seismic imaging, Geophysics 55: 626-623, 1990

Richmond, J.H., Scattering by a dielectric cylinder of arbitary cross section shape, IEEE Trans, Ant. Prop. 13:334-341, 1965

Steven A. Johnson and Michael L. Tracy, Inverse Scattering solution by a sinc basis, multiple source, moment method --Part I : Theory, Ultrosonic Imaging 5, 361-375, 1983

Weng Chow Chew and Cai-cheng Lu, The use of Huygens' Equivalence principle for solving the volume integral equation of scattering, IEEE Transaction on antennas and propagation, vol. 41, no.7, 897-904,1993